# Adaptive Scene-Based Non-Uniformity Correction Method for Infrared-Focal Plane Arrays

Sergio N. Torres, Esteban M. Vera, Rodrigo A. Reeves, Sergio K. Sobarzo

Department of Electrical Engineering
University of Concepcion, Chile

## ABSTRACT

The non-uniform response in infrared focal plane array (IRFPA) detectors produces corrupted images with a fixed-pattern noise. In this paper we present an enhanced adaptive scene-based non-uniformity correction (NUC) technique. The method simultaneously estimates detector's parameters and performs the non-uniformity compensation using a neural network approach. In addition, the proposed method doesn't make any assumption on the kind or amount of non-uniformity presented on the raw data. The strength and robustness of the proposed method relies in avoiding the presence of ghosting artifacts through the use of optimization techniques in the parameter estimation learning process, such as: momentum, regularization, and adaptive learning rate. The proposed method has been tested with video sequences of simulated and real infrared data taken with an InSb IRFPA, reaching high correction levels, reducing the fixed pattern noise, decreasing the ghosting, and obtaining an effective frame by frame adaptive estimation of each detector's gain and offset.

**Keywords:** Focal-Plane Array, Non-Uniformity Correction, Neural Networks, Fixed-Pattern Noise.

## 1. INTRODUCTION

The majority of the infrared imaging sensors are based on the Infrared Focal Plane Array (IRFPA) technology.[1,2] This leading-edge technology consists of an array of independent infrared detectors. Unfortunately, every detector in the array has unequal responses under the same stimulus, which leads to the presence of a fixed-pattern noise on the resulting images.

The best calibration methods for the Non-Uniformity Correction (NUC) of an IRFPA are based on the use of uniform infrared sources. These methods are denominated as Reference-Based NUC techniques. The most used one is the *Two-Point Calibration* method, which employs at least two blackbody sources at different temperatures to calculate the gain and the offset of each detector on the IRFPA. Unfortunately, such kinds of NUC methods require to halt the normal operation of the system, and they also need a very expensive setup.

For these reasons, Scene-Based NUC techniques are actually becoming more popular, since they only need the readout infrared data captured by the imaging system during its normal operation, in order to compensate for the non-uniform response. The scene-based technique most referred is the one based in the constant statistics constraint.[3,4] Nonetheless, several other sophisticated methods have been recently proposed in the literature.[5–9]

Nevertheless, all of the cited Scene-Based NUC techniques make the assumption that all the detector's parameters remain constant over a certain block of frames, and thus their performance could be affected by the detector's parameters drift. Clearly, none of such techniques adapts sensor's parameters over time under a frame by frame basis. The first approach in this way was developed in,[10,11] where a retina-like neural net was used to perform the non-uniformity compensation. This is what we meant by an adaptive NUC technique, which consists of an array of linear neurons that are connected to each detector's output, acting as the inverse model for each detector. The parameters of the neurons (bias and weight) are updated through a steepest descent linear regression, using a local averaging of their outputs as the desired outputs for each neuron. These neuron parameters are equivalent to the original detector's parameters offset and gain.

---

Further author information:
Sergio N. Torres: E-mail: storres@die.udec.cl, Telephone: (+56-41)203005, Address: Casilla 160-C, Concepcion, Chile.

Normally this adaptive NUC algorithm performs well, but as stated in,[12] sometimes it produces severe ghosting artifacts on the output images. For this reason, a brief study on the origin of such artifacts are discussed in this paper, and then an enhanced version of the Scribner's[11] NUC method is proposed. The proposed improvements to the algorithm are mainly based on the addition of some optimization techniques to the steepest descent algorithm,[13] which is used to perform the adaptive detector's parameter estimation process. Specifically, the enhanced adaptive NUC method here proposed uses the addition of: $1^{st}$, a momentum[14] term for stabilizing and accelerating the learning process; $2^{nd}$, a regularization[15] term for balancing the parameters update process; and $3^{rd}$, an adaptive learning rate schedule. This adaptive learning rate is dependent on the conditions of the input data. Then the adaptation speed of the learning process for a given pixel can be increased in a confident way, allowing a possible better and faster non-uniform correction performance with probably less ghosting artifacts.

This paper is organized as follows. In Section 2 the adaptive NUC technique is developed, and its enhancements detailed. In Section 3 the proposed NUC technique is tested with sequences of infrared data with simulated nonuniformity. In Section 4 the technique is applied to sequences of real infrared data. The conclusions of the paper are summarized in Section 5.

## 2. ADAPTIVE SCENE-BASED NUC METHOD

Usually, an infrared detector is characterized by a linear model. Then, for the $(ij)^{\text{th}}$ detector in the focal plane array, the measured readout signal $Y_{ij}$ at a given time $n$ can be expressed as:

$$Y_{ij}(n) = a_{ij}(n) \cdot X_{ij}(n) + b_{ij}(n) \tag{1}$$

where $a_{ij}(n)$ and $b_{ij}(n)$ are the gain and the offset of the $ij^{\text{th}}$ detector, and $X_{ij}(n)$ is the real incident infrared radiation collected by the respective detector. The main idea of the NUC scene-based methods relies in estimating the gain and the offset parameters of each detector on the IRFPA using only the readout data $Y_{ij}(n)$. In the particular case of Scribner's NUC method,[10, 11] the algorithm has the ability of adapting sensor's parameters over time under a frame by frame basis. To understand how the neural network based approach proposed by Scribner works, equation (1) must be reordered as follows:

$$X_{ij}(n) = g_{ij}(n) \cdot Y_{ij}(n) + o_{ij}(n) \tag{2}$$

where the new parameters $g_{ij}(n)$ and $o_{ij}(n)$ are related to the real gain and offset parameters of the detectors, as expressed in the following expressions:

$$g_{ij}(n) = \frac{1}{a_{ij}(n)} \qquad o_{ij}(n) = -\frac{b_{ij}(n)}{a_{ij}(n)} \tag{3}$$

In this way, the expression presented in equation (2) is responsible of performing the non-uniformity correction of the readout data, but it will only be successful in this task if the parameters involved are well identified.

### 2.1. General Algorithm Description

The parameters of the linear model presented in eq.(2) can be estimated using linear regression. Therefore, if the parameters are adaptive too, the non-uniformity correction model in (2) can also be considered as the simplest neural network structure, which consists on a single neuron with one weight $g_{ij}(n)$ and a bias $o_{ij}(n)$. The readout data $Y_{ij}$ is the input to this neuron, then its output $\hat{X}_{ij}(n)$ can be obtained as follows:

$$\hat{X}_{ij}(n) = \hat{g}_{ij}(n) \cdot Y_{ij}(n) + \hat{o}_{ij}(n) \tag{4}$$

where the parameters $\hat{g}_{ij}$ and $\hat{o}_{ij}$ must be recursively updated in order to minimize some error function that allows a good estimation for the real infrared data represented by $\hat{X}_{ij}$.

Then, to perform the parameter estimation using linear regression, the error function $E_{ij}(n)$ for each neuron is usually defined as the difference between a desired target value $T_{ij}(n)$ and the estimated infrared data $\hat{X}_{ij}$ (5).

Using a biological inspired approach,[11] the target value needed to estimate the unknown parameters for NUC purposes, can be calculated as the local spatial average (mean filter) of the output data $\hat{X}_{ij}$.

$$E_{ij}(n) = T_{ij}(n) - \hat{X}_{ij}(n) \tag{5}$$

Thus, to minimize the error $E_{ij}(n)$ in the mean square error sense, a functional $J$ is defined as follows:

$$J_{ij} = \sum_n E_{ij}(n)^2 = \sum_n (T_{ij}(n) - \hat{X}_{ij}(n))^2 \tag{6}$$

Then, the corresponding gradients relatives to each parameter are obtained in 7.

$$\frac{\partial J_{ij}}{\partial \hat{g}_{ij}} = -2 \cdot E_{ij} \cdot Y_{ij} \tag{7}$$
$$\frac{\partial J_{ij}}{\partial \hat{o}_{ij}} = -2 \cdot E_{ij}$$

However, the functional $J$ is minimized only when its both partial derivatives (or gradients) in equation (7) are equal to 0. A good way to solve this Least Mean Square (LMS) optimization problem is through the well known steepest descent algorithm.[13] In this gradient-based search algorithm, the parameters to be estimated are recursively and smoothly updated with a portion of each respective error gradient. The parameter update procedure, or learning process, is finally described as follows:

$$\hat{g}_{ij}(n+1) = \hat{g}_{ij}(n) - \eta \cdot E_{ij}(n) \cdot Y_{ij}(n) \tag{8}$$
$$\hat{o}_{ij}(n+1) = \hat{o}_{ij}(n) - \eta \cdot E_{ij}(n)$$

where $\eta$ is a fixed parameter known as the learning rate.

## 2.2. Proposed Enhancements

During the adaptation process of the weight parameters $\hat{g}_{ij}(n)$, their estimated values usually tend to get unbalanced from the desired unitary mean, mainly due to its dependence on the input data (8). As a consequence, an unbalance of the bias parameters $\hat{o}_{ij}(n)$ is also produced (in this case the unbalance is from its desired zero mean), because the bias parameters try to compensate the unbalance on the weight parameters. Thus, a slower convergence of the estimation process is expected.

A proper parameters balance can be achieved with the addition of a regularization term $r(n)$, like the one proposed in eq.(9), where $\lambda$ is the regularization constant and where $N \times M$ is the number of pixels on the IRFPA. This $r$ term adds in a soft way a constraint that forces all the weight values in the array to have a unitary mean. It must be only added to the weight update equation in (8).

$$r(n) = \lambda \cdot (1 - \frac{1}{NM}(\sum_{i=1}^{N}\sum_{j=1}^{M}\hat{g}_{ij}(n))) \tag{9}$$

Another possible enhancement to the steepest descent algorithm is the well known momentum. It is mainly used in more complex neural network structures to avoid the local minima problem. Since the particular model used here to solve the non-uniformity correction is linear, it seems that no local minima exists. However, sometimes the desired target value of the algorithm is not as good as one could wish, and thus the normal steepest descent algorithm presents a local minima-like behavior. Therefore, the use of momentum could improve the performance of the adaptive algorithm, improving its stability and probably reducing the production of ghosting artifacts.

If the momentum term is added to the parameters update equation (8), then the learning procedure can be rewritten as follows:

$$\hat{g}_{ij}(n+1) = \hat{g}_{ij}(n) - \eta \cdot E_{ij}(n) \cdot Y_{ij}(n) + \alpha \cdot (\hat{g}_{ij}(n) - \hat{g}_{ij}(n-1)) \tag{10}$$
$$\hat{o}_{ij}(n+1) = \hat{o}_{ij}(n) - \eta \cdot E_{ij}(n) + \alpha \cdot (\hat{o}_{ij}(n) - \hat{o}_{ij}(n-1))$$

where $\alpha$ is the momentum constant that usually varies between 0.1 and 0.9 to assure stability.

The final enhancement proposed to the steepest descent learning process is the use of an adaptive learning rate schedule. The main idea behind the use of an adaptive learning rate is trying to increase the convergence speed as much as it is possible. In the particular case of the adaptive NUC, an adaptive learning rate must also tries to control the production of ghosting artifacts. Usually, the stability given when a momentum term is used, allows a robust increase on the learning rate. So, when momentum and regularization are both used, the inclusion of an adaptive learning rate scheduling can be tried in a safer way.

Thus, based on the knowledge that the local spatial average is not always a good estimate for the desired target response of an adaptive NUC method, the proposed adaptive learning rate $\eta_{ij}(n)$ showed in eq.(4), is designed to be dependent, and inversely proportional to the local spatial variance of the input image $\sigma^2_{Y_{ij}}(n)$.

$$\eta_{ij}(n) = K * \frac{1}{1 + \sigma^2_{Y_{ij}(n)}} \tag{11}$$

Therefore, if a given piece of the input image (a pixel and its neighbors) is smooth enough, then the desired averaged target value at the output is more confident, and the learning rate gets larger value. On the other hand, if the local input variance in the surroundings of a certain pixel is too high, like in a object border, the learning rate gets a slower value. To add this adaptive learning rate to the adative NUC algorithm, $\eta$ in equation (8) must be replaced by its counterpart $\eta_{ij}(n)$ in (11), where $K$ is a constant that regulates the maximum learning rate allowed. The local variance $\sigma^2_{Y_{ij}}(n)$ can be calculated with any desired window size, maybe dependent on the window size also used to calculate the local average for the desired output. However, a $3 \times 3$ window size will be assumed along this paper.

## 3. APPLICATIONS TO SIMULATED INFRARED DATA

In this section, the proposed enhancements to the Scribner's adaptive NUC method are tested with infrared data corrupted with simulated non-uniformity. The infrared sequences with artificial non-uniformity were generated from a clean 3000 frame infrared video sequence, according to procedures like the ones presented in.[9, 16] Then, several 3000 frame corrupted video sequences were obtained using a synthetic gain with an unitary- mean gaussian distribution with 3% of variance, and a synthetic offset with a zero-mean gaussian distribution with 5% of variance. As an example, Figure 2a) shows a true infrared image and Figure 2b) shows the corresponding corrupted one. The parameters used to initialize the weight and bias estimation process are 1 and 0 respectively.

### 3.1. Performance Metrics

To study the performance of the proposed enhanced methods, we employ the Pseudo Signal To Noise Ratio (PSNR) performance metric, which is based on the Root Mean Square Error (RMSE). The PSNR is expressed in dB and it is defined as follows:

$$RMSE = \sqrt{\frac{1}{NM} \sum_{ij} (I_{ij} - \hat{I}_{ij})^2} \tag{12}$$

$$PSNR = 20 \cdot log_{10} \left( \frac{2^b}{RMSE} \right) \tag{13}$$

where $I_{ij}$ is the $ij$ pixel value of the true frame, and $\hat{I}_{ij}$ is $ij$ the pixel value of the corrected frame. The frame size is $N \times M$ pixels, and $b$ represents the number of bits per pixel in the image, which in this case is equal to 8 for all the simulations. The PSNR values shown in this section were computed averaging the results obtained after 50 trials. As an example, the PSNR of the corrupted image sequences with simulated non-uniformity are about 26dB for all the frames. Larger values for the PSNR indicates better performances.
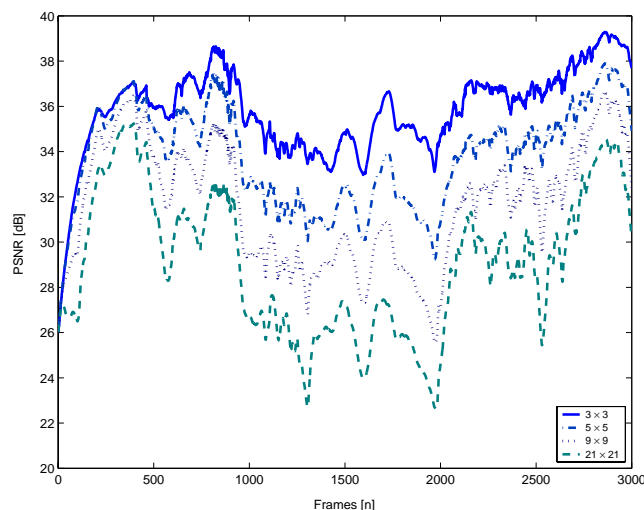
**Figure 1.** Impact of changing the averaging window size on the performance of Scribner's adaptive NUC method.

## 3.2. Averaging Window Size Analysis

First, we have tested the performance of Scribners method with different sizes in the averaging window used to calculate the reference for each neuron desired output. For this purpose, the learning rate was fixed at $\eta = 0.01$, and the window size was changed between $3 \times 3$ until $21 \times 21$. The results are displayed in Figure 1, where it is clear that the use of a $3 \times 3$ local averaging window is much better than the use of any larger window sizes such as the $21 \times 21$ used by Scribner.[11]

From the analysis of the single frame presented in Figure 2c) and d), where c) shows the corrected image with an averaging window of $3 \times 3$ and d) the corrected image with an averaging window of $21 \times 21$, it's easily noticeable the improvement on the quality of the corrections performed by the smaller window size, with a great reduction in the amount of ghosting artifacts that appears when the larger window is used. This conclusion is also reaffirmed when the video sequences are watched as a movie. This results leads to the selection of the $3 \times 3$ local averaging window to be used in all the remaining simulations presented in this paper.



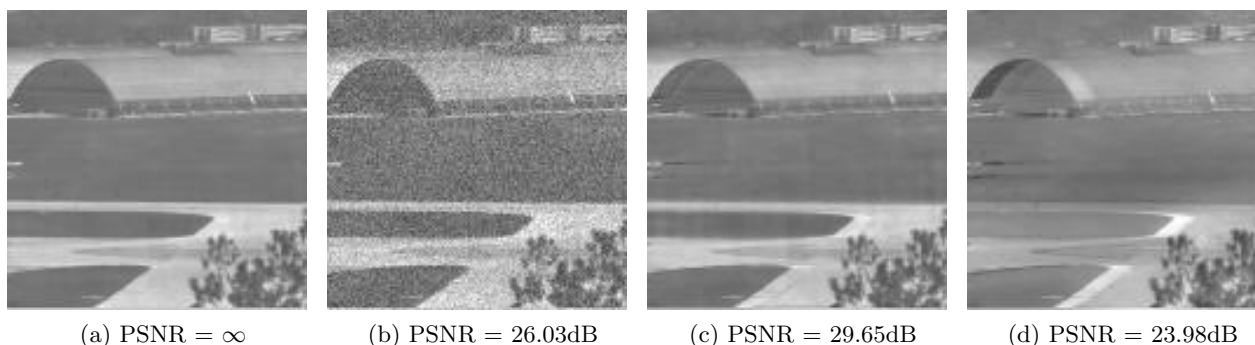| (a) PSNR = $\infty$ | (b) PSNR = 26.03dB | (c) PSNR = 29.65dB | (d) PSNR = 23.98dB |

**Figure 2.** Impact of changing the averaging window on the performance of the Scribner's adaptive NUC method for frame 1600 of the image sequence. a) The true frame. b) The corrupted frame. c) The corrected frame with $\eta = 0.01$ and a window size of $3 \times 3$. d) The corrected frame with $\eta = 0.01$ and a window size of $21 \times 21$.

## 3.3. Learning Rate Analysis

In order to get familiarized with the strengths and weakness of the proposed enhanced adaptive NUC, we start performing simulations using the simulated corrupted video sequence using several fixed values for the learning

rate $\eta$. For all these $\eta$ values, the performance parameters PSNR for Scribner's NUC method, and for three of the proposed improvements to the adaptive NUC method were calculated. The PSNR is presented as an average value over the whole video sequence in Figure 3a), and as the obtained value for a given sample frame in Figure 3b).
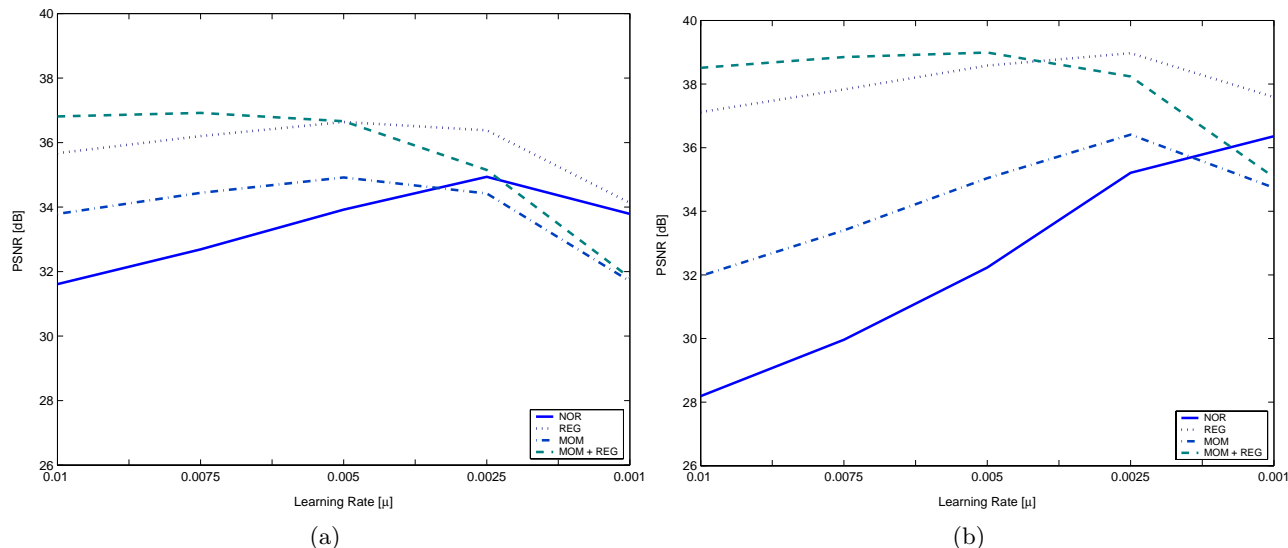


(a)  (b)

**Figure 3.** PSNR for the Adaptive NUC algorithm and its proposed modifications versus learning rate $\eta$. a) Mean PSNR for the whole sequence. b) PSNR for selected frame 2600. 'NOR' indicates Scribner's method, 'MOM' indicates Scribner's method plus momentum, 'REG' indicates Scribner's method plus regularization, and 'MOM+REG' indicates Scribner's methos plus momentum and regularization.

In the graphics presented at figure 3a), the method which uses regularization presents a better performance than Scribner's for all the $\eta$ range shown on the figure. Additionally, the method using momentum, only seems to perform well at larger learning rates. Also, it can be said that at lower learning rates the proposed improvements based on the addition of momentum, and momentum plus regularization, generate a smaller PSNR than the Scribner's method. Anyway, for the later cases, the best possible PSNR values are reached using learning rates greater than $\eta = 0.005$. Figure 3b) show similar results for a particular frame in the sequence, but there the performance improvements of the proposed enhancements to the Scribner's method are even more noticeable. From the both graphics, the best performance is achieved when momentum and regularization are used together with a learning rate of $\eta = 0.005$.

### 3.4. Adaptive Learning Rate Analysis

In this subsection, we have studied the performance of the complete proposed enhanced method, using an adaptive learning rate schedule which also uses momentum and regularization. To perform a proper comparison, a value of $\eta = 0.005$ was chosen for the fixed learning rate techniques counterparts, including the Scribner's NUC method and its modified enhancements such as momentum, and momentum plus regularization.

In figure 4, it can be seen that when the adaptive learning rate is used, it outperforms all the fixed learning rate techinques from the frame 1000 until the last frame, where the improvement is even more noticeable. From the same graphic, it can be noticed that the proposed improvements used with the fixed learning rate approach outperforms the original Scribner's NUC method over almost the whole frame sequence.

As example, the frame 1300 of the simulated infrared sequence, shown in figure 5a), is compensated with Scribner's method in figure 5c) and with the adaptive learning rate method in figure 5d). The PSNR computed for the adaptive learning rate method is 4dB greater than the one computed on the frame compensated with the Scribner's method, and it is almost 12dB over the PSNR level of the corrupted infrared sequence. Furthermore,
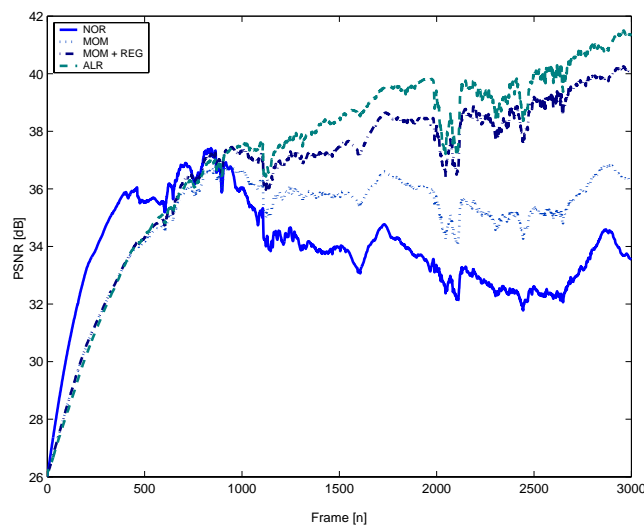
**Figure 4.** Comparison of PSNR versus frame time for the adaptive learning rate and fixed learning rate $\eta = 0.005$.'NORMAL indicates Scribners NUC method, 'MOM indicates the use of the momentum term, 'MOM + REG indicates the use of the momentum and the regularization term, 'ALR indicates the use of an adaptive learning rate schedule using the momentum and the regularization term.

watching the correspondent movie sequences with the naked eyes, it can be seen that the adaptive learning rate method noticeably generates less ghosting artifacts than the Scribner's method, which explains in part the higher performance rates achieved.
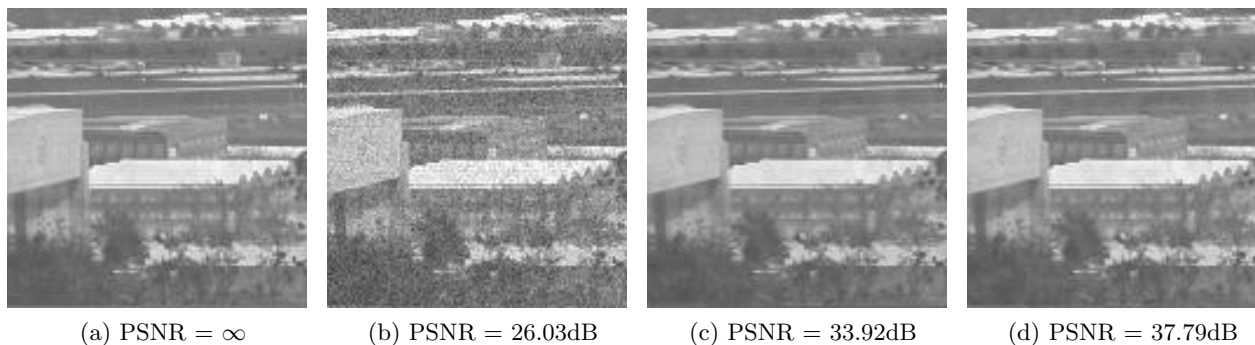


(a) PSNR $= \infty$      (b) PSNR $= 26.03$dB      (c) PSNR $= 33.92$dB      (d) PSNR $= 37.79$dB

**Figure 5.** Frame 1300 of the infrared sequence. a) True infrared image; b) Corrupted image; c) Corrected image with Scribners NUC method; d) Corrected image with the proposed NUC method using adaptive learning rate plus momentum and regularization.

## 4. APPLICATIONS TO REAL INFRARED DATA

The Scribner's adaptive NUC algorithm, and all the proposed improvements were applied to several data sequences of real IR data. The data were collected by using a 16-bit 128 InSb FPA camera (Amber model AE-4128), operating in the 3-5$\mu$m range. The available data sequences were taken at 8:00 A.M., 9:30 A.M. and at 1:00 P.M. Blackbody measurements are also available to perform the two-point calibration on the 1:00 P.M. image sequence.

The performance metric PSNR is used again to compare the results obtained on the 1:00 P.M. data using Scribner's method and the adaptive learning rate. In this case, the initial parameters used for the weight and

bias estimation are 1 and 0 respectively. On the other hand, the remaining sequences are used to check the adaptability capacity of the adaptive learning rate method, changing from one block of data to the other.

As a first analysis, the learning rate of $\eta = 0.005$ used in previous simulations was chosen to perform the comparisons. Figure 6 shows the performance parameter PSNR over the whole 1:00 P.M. real infrared sequence. Note that the adaptive learning rate method, with momentum plus regularization, achieves the best performance through most of the sequence.
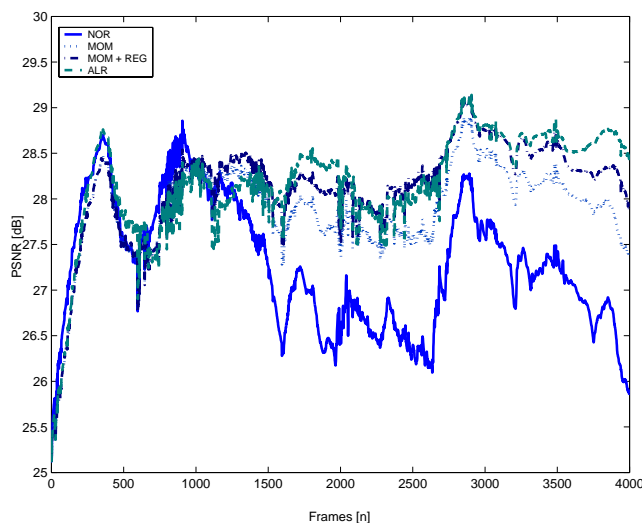


**Figure 6.** Comparison of PSNR versus frame time for the adaptive learning rate and fixed learning rate $\eta = 0.005$.'NORMAL indicates Scribners NUC method, 'MOM indicates the use of the momentum term, 'MOM + REG indicates the use of the momentum and the regularization term, 'ALR indicates the use of an adaptive learning rate schedule using the momentum and the regularization term.

When a sample frame is analyzed, like the one shown in figure 7, it can be seen that when the adaptive learning rate is used (figure 7d)), most of the ghosting artifacts that appears when the Scribner's method is used (figure 7c)) are avoided. However, the adaptive learning rate procedure presents noticeable problems with dead and saturated pixels, while Scribner's method removes them. These results are reaffirmed when the corresponding video sequences are observed. Also, from the same video sequences it must be commented that the adaptive learning rate algorithm performs in an outstanding way.
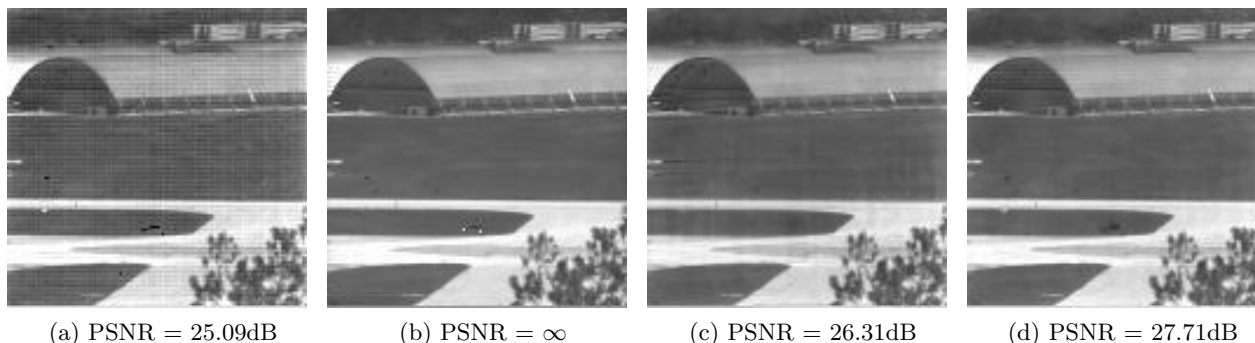


|  (a) PSNR = 25.09dB | (b) PSNR = $\infty$ | (c) PSNR = 26.31dB | (d) PSNR = 27.71dB |

**Figure 7.** Frame 1600 of the 1:00 P.M. real infrared sequence. a) True infrared image; b) Corresponding corrupted image; c) Corresponding corrected image with Scribners NUC method; Corresponding corrected image with the proposed NUC method using adaptive learning rate plus momentum and regularization.

The final analysis performed with real data is based on observing if the adaptive learning rate method is able to follow the drift between blocks of data taken at different times. If the NUC algorithm follows the drift, the updated parameters should compensated the fixed-pattern noise without ghosting. On the other hand, if the NUC algorithm doesn't perform well, the parameters are contaminated with previous image information showing ghosting artifacts.
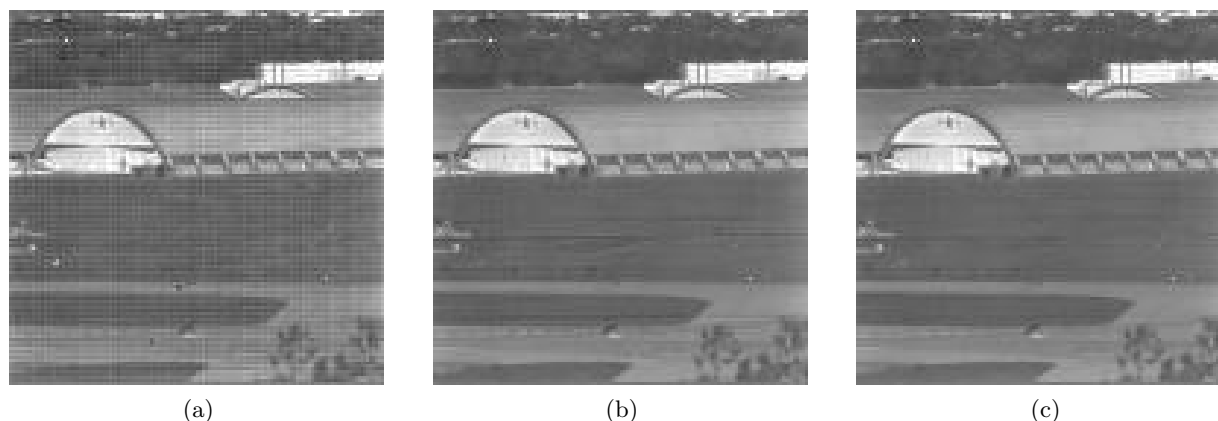


(a)          (b)          (c)

**Figure 8.** frame 1 of the real infrared sequence taken at 9:30 A.M. a) Corrupted readout frame. b) Corrected frame with Scribner's method using momentum plus regularization. c) Corrected frame using adaptive learning rate with momentum plus regularization.

As an example, the adaptive learning rate method and the Scribner's method are applied to two sequences of infrared raw data separate one and a half hour (8:00 and 9:30 AM). Figure 8 shows the first frame of the 9:30 A.M. data sequence with the corresponding compensated versions using Scribner's method with momentum and regularization and the adaptive learning rate algorithm. Note the presence of strange shadows (ghosting) on the frame compensated by the Scribner NUC method plus momentum and regularization. However, the frame compensated by the adaptive learning rate does not contain such shadows.

## 5. CONCLUSIONS

We have developed an enhanced adaptive scene-based NUC method based on the Scribner's adaptive NUC technique. Such technique is improved by the addition of several optimization techniques such as momentum, regularization, and adaptive learning rate, all applied to the steepest descent algorithm.

We also have proposed another enhancement derived from our first experiment with simulated data, where we have concluded that a better performance can be expected if a smaller averaging window, such as a $3 \times 3$ one, is used to calculate the desired target for the adaptive algorithm.

After several simulations, with simulated and real corrupted infrared data, we have concluded that the addition of the momentum and the regularization term always helps in increasing the quality of the non-uniformity corrections of the adaptive NUC method. The overall performance is even better if both techniques are employed together. However, when both techniques are used, the ghosting artifacts weren't entirely removed.

Nonetheless, when the adaptive learning rate scheduling is also introduced, the obtained results were outstanding when compared to all the other methods tested. Also, its ability in avoiding the production of ghosting artifacts is impressive. Furthermore, it was shown using sequences of raw data separated by one hour and a half that the sum of the proposed enhancements are able to track the drift in the parameters responsible of the fixed-pattern noise. Finally, from all the above it is concluded that the adaptive learning rate scheduling is a promissory algorithm to perform non-uniformity correction on IRFPA-based systems in an adaptive frame-by-frame basis.

Further research may include studies on the use of temporal variance information of the input data to improve even more the performance of the adaptive learning rate here proposed.

## Acknowledgments

## REFERENCES

1. D. Scribner, M. Kruer, and J. Killiany, "Infrared focal plane array technology," *Proceedings of the IEEE* **79**(1), pp. 66–85, 1991.
2. G. Holst, *CCD Arrays, Cameras and Displays*, SPIE Optical Engineering Press, Bellingham, 1996.
3. P. Narendra, "Reference-free nonuniformity compensation for ir imaging arrays," *Proceedings of SPIE* **252**, pp. 10–17, 1980.
4. J. Harris and Y. Chiang, "Nonuniformity correction of infrared image sequences using the constant-statistics constraint," *IEEE Transactions on Image Processing* **8**, pp. 1148–1151, August 1999.
5. M. Hayat, S. Torres, E. Armstrong, S. Cain, and B. Yasuda, "Statistical algorithm for nonuniformity correction in focal-plane arrays," *Applied Optics-IP* **38**, pp. 772–780, February 1999.
6. R. Hardie, M. Hayat, E. Armstrong, and B. Yasuda, "Scene-based nonuniformity correction with video sequences and registration," *Applied Optics-IP* **39**, pp. 1241–1250, March 2000.
7. S. Cain, M. Hayat, and E. Armstrong, "Projection-based image registration in the presence of fixed-pattern noise," *IEEE Transactions on Image Processing* **10**, pp. 1860–1872, December 2001.
8. B. Ratliff, M. Hayat, and R. Hardie, "An algebraic algorithm for nonuniformity correction in focal-plane arrays," *Journal of the Optical Society of America A* **19**(9), pp. 1737–1747, 2002.
9. S. Torres and M. Hayat, "Kalman filtering for adaptive nonuniformity correction in infrared focal-plane arrays," *Journal of the Optical Society of America A* , pp. 470–480, March 2003.
10. D. Scribner, K. Sarkady, M. Kruer, J. Caulfield, J. Hunt, M. Colbert, and M. Descour, "Adaptive nonuniformity correction for ir focal plane arrays using neural networks," *Proceeding of the SPIE* **1541**, pp. 100–109, 1991.
11. D. Scribner, K. Sarkady, M. Kruer, J. Caulfield, J. Hunt, M. Colbert, and M. Descour, "Adaptive retina-like preprocessing for imaging detector arrays," *Proceedings of the IEEE International Conference on Neural Networks* **3**, pp. 1955–1960, 1993.
12. E. Vera, R. Reeves, and S. Torres, *Soft Computing Systems: Design, Management and Applications*, ch. Adaptive Bias Compensation for Non-Uniformity Correction on Infrared Focal Plane Array Detectors, pp. 725–734. IOS Press, 2002.
13. J. Principe, N. Euliano, and W. C. Lefebvre, *Neural and Adaptive Systems*, John Wiley & Sons, 2000.
14. S. Haykin, *Neural Networks: A Comprehensive Foundation*, Prentice Hall, 1998.
15. J. Sjoberg, *Artificial Intelligence in Real-Time Control*, ch. Regularization as a Substitute for Pre-Processing of Data in Neural Network Training, pp. 31–35. Elsevier Science, 1992.
16. S. Tzimopoulou and A. Lettington, "Scene based techniques for nonuniformity correction of infrared focal plane arrays," *Proceedings of the SPIE* , pp. 172–183, 1998.